# Interference of nematic quantum critical quasiparticles: A route to the octet model

Eun-Ah Kim[1] and Michael J. Lawler[2,1]
[1]*Department of Physics, Cornell University, Ithaca, New York 14853, USA*
[2]*Department of Physics, Binghamton University, Binghamton, New York 13902, USA*
(Received 1 March 2010; published 2 April 2010)

We study the effect of nematic quantum critical fluctuations on quasiparticle interference. We show that nematic quantum critical fluctuations, which cause back and forth slushing of the *d*-wave nodes along the underlying Fermi surface, provide a natural mechanism for the accumulation of coherence that has been present in QPI experiments.

DOI: 10.1103/PhysRevB.81.132501 PACS number(s): 74.20.De, 73.43.Nq, 74.25.Dw, 74.72.−h

Interference effects[1–4] suggest that the low-energy quasiparticles (qp's) in cuprate superconductors can maintain coherence under special circumstances. Such coherence is at odds with observations of inhomogeneity at higher energy scales.[5–8] In particular, quasiparticle interference (QPI) imaging using scanning tunneling spectroscopy revealed a unusual form of coherence: accumulation of coherence only at special points in momentum space (so-called "tip of banana").[1,2,8] The simplicity of the QPI image, a set of well-defined dispersing peaks, is striking considering the complexity of the real-space image.[1] made an insightful observation: the peak positions are determined by the eight tips of the "banana" shaped qp equal-energy contours. However, a key question remains of this "octet model"—what makes the qp's at the tips especially coherent to the extent that only interference among qp's at the tips remain visible.

Underlying the QPI interpretation of the Fourier transform of the LDOS map $N(\vec{r},\omega)$ is the assumption that the modulated contribution $\tilde{N}_{imp}(\vec{q},\omega)$ results from coherent qp's scattering off sparsely distributed impurities. For conventional metals where these assumptions hold, the modulations in LDOS can be understood in terms of interference among single-particle wave functions.[11,12] However simple models for the QPI in cuprates also in terms of free (Bogoliubov) qp pictures[12–15] predict extended patterns which only overlap with experiments at special points and efforts to resolve this discrepancy have been focused on fine tuning nature of scatters in models[16] or proposed description of pseudogap phase.[17] Here we show that a proximity to the nematic quantum critical point (QCP) of a *d*-wave superconductor can provides a robust mechanism for octet model without fine tuning.

We start by noting that QPI phenomenology is missing a scattering mechanism that discriminates banana tips from the rest. Recently, it has been shown[9] that critical fluctuations near the nodal nematic QCP have the correct symmetry to introduce such additional scattering from strong correlation effect. "Nematic" here refers to a broken-symmetry phase in which the fourfold rotational symmetry of the crystal is broken down to a twofold symmetry [see Fig. 1(a)]. In a *d*-wave superconductor, such additional symmetry-breaking results in a shifting of the nodal positions away from their fourfold symmetric locations.[18] At the nodal nematic QCP, we found[9] that the softening of the nodal positions introduces strongly $\vec{k}$ dependent decoherence that brings in stark contrast between the tips, where qp's remain coherent with long lifetime, and the rest of the equal-energy contour, where qp's get severely damped [see Figs. 1(b) and 1(c)].

Our results show that $\vec{k}$ dependent decoherence due to nematic fluctuations can explain QPI peaks in Fourier transform LDOS. We further argue for the uniqueness of this route based on (1) the severely restricted qp scattering

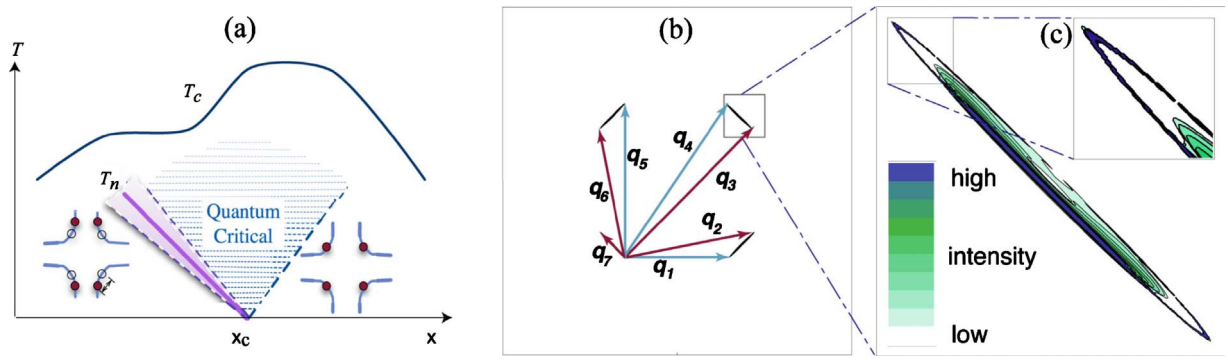


FIG. 1. (Color online) The electron spectral distribution at the nodal nematic quantum critical point in the linearized approximation (taken from Ref. 9). (a) proposed phase diagram inside the superconducting dome, where *x* is a tuning parameter. Note the change in location of the nodes through the phase transition. (b) Equal energy contour at $\omega=3$ meV and the connecting $\vec{q}$ vectors of the banana tips. The $\vec{q}_i$ are colored blue and red depending on whether they connect $\vec{k}$ points with the same or opposite sign of the *d*-wave gap $\Delta_{\vec{k}}$. (c) blowup of the momentum distribution $A(\vec{k},\omega=3$ meV) of the spectral function near one node. Note the sharpness of the momentum distribution at the banana tip shown in the inset.

 

mechanisms in a *d*-wave superconductor due to their limited phase space[18] and on (2) direct evidence for nematic ordering in underdoped cuprates.[19] Also, both the glassy nematic behavior in underdoped $Bi_2Sr_2CaCu_2O_{8+\delta}$ (Ref. 8) and the doping dependent flattening of the near-node gap slope $Bi_2Sr_2CaCu_2O_{8+\delta}$ (Refs. 2 and 20–22) are consistent with increasing degree of nematicity upon underdoping.

In a many-body setting, one can capture the modulation of local density of states (LDOS) resulting from isolated impurities using the T-matrix formalism (see for example Ref. 15) which expresses the energy resolved LDOS $\tilde{N}_{imp}(\vec{q},\omega)$ at wave vector $\vec{q}$ as

$$\tilde{N}_{imp}(\vec{q},\omega) = -2\ \mathrm{sgn}(\omega)\mathrm{Im}\int d\vec{k}[\hat{\mathcal{G}}(\vec{k}+\vec{q},\omega)\hat{T}\hat{\mathcal{G}}(\vec{k},\omega)]_{11} \tag{1}$$

where $\hat{\mathcal{G}}(\vec{k},\omega)$ is the $(2\times 2)$ single-particle Nambu matrix propagator in a superconducting state without impurity scattering and $\hat{T}$ is the impurity potential in the weak (perturbative) impurity limit. Here $\hat{T}$ depends on the type of impurity. For a charge impurity which is antisymmetric in Nambu space, $\hat{T}=V_c\hat{\sigma}_3$, while $\hat{T}=V_m\mathbb{I}$ for a magnetic impurity and $\hat{T}=V_\Delta\hat{\sigma}_1$ for a *d*-wave superconducting gap impurity (which has momentum dependence[23,24]), both of which are symmetric in Nambu space ($\hat{\sigma}_i$ are Pauli matrices acting on Nambu spinors).

Clearly $\tilde{N}_{imp}(\vec{q},\omega)$ in Eq. (1) is the amplitude modulation for the overlap between two qp states with wave vector $\vec{k}$ and $\vec{k}+\vec{q}$ scattering off the impurity. Hence high intensity in $\tilde{N}_{imp}(\vec{q},\omega)$ require given $\vec{q}$ to connect high density of *coherent* (long-lived) qp states. McElroy *et al.*[1] and Wang and Lee[13] noticed that the spectral density Im $\hat{\mathcal{G}}$ is accumulated at the $\vec{k}$ points at the eight tips of the "banana" contours. Further, autocorrelation analysis of ARPES spectra which measures spectral weight supported this phenomenological connection.[26] However, this similarity is not reproduced by calculations of relevant quantities. Hence peaks observed in QPI requires a mechanism that brings special coherence to the tips as well as enhanced spectral weight. Such a mechanism has been unknown.

The nature of the propagating single qp states is encoded in the Nambu matrix propagator $\hat{\mathcal{G}}$ entering Eq. (1). If, in between impurity scattering events, the qp's experience collisions with critical nematic collective modes, a self-energy $\hat{\Sigma}$ is induced (see, e.g., Ref. 27)

$$\hat{\mathcal{G}}^{-1} = \hat{\mathcal{G}}_0^{-1} - \hat{\Sigma}. \tag{2}$$

Here $\hat{\mathcal{G}}_0$ is the free Bogoliubov qp propagator of a BCS superconductor. In order to capture the nematic critical fluctuations, we use the self-energy defined in Ref. 9 (see also below). In the context of the cuprates, $\hat{\mathcal{G}}_0(\vec{k},\omega)$ takes the form

$$\hat{\mathcal{G}}_0^{-1} = (\omega+i\delta)\mathbb{I} - \varepsilon_{\vec{k}}\sigma_3 - \Delta_{\vec{k}}\sigma_1 \tag{3}$$

where $\varepsilon_{\vec{k}}$ is the dispersion of the normal-state qp's and $\Delta_{\vec{k}} = \Delta_0(\cos k_x a - \cos k_y a)$ is the *d*-wave pairing amplitude. In the low energy long-wavelength limit, we can approximate this $\hat{\mathcal{G}}_0$ by linearizing around the four gapless nodal points $\vec{k}\approx\vec{K}$ where the qp energy $\xi_{\vec{k}}=\sqrt{\varepsilon_{\vec{k}}^2+\Delta_{\vec{k}}^2}$ vanishes,

$$\mathcal{G}_0^{-1}|_{\text{near node }\vec{K}} = (\omega+i\delta)\mathbb{I} - v_F(k_x-K_x)\hat{\sigma}_3 - v_\Delta(k_y-K_y)\hat{\sigma}_1. \tag{4}$$

Linearizing $\varepsilon_{\vec{k}}$ and $\Delta_{\vec{k}}$ given in Ref. 28 based on photoemission data, we find $v_F=0.508$ and $v_\Delta=0.025$ in units of $eV(a/\pi)$. (Note that the resulting anisotropy ratio $v_F/v_\Delta = 20.3$ is large and consistent with the value of 19 inferred from thermal-conductivity measurements.[10])

Intuitively one can understand angle dependence of the nematic fluctuation effects from transverse gauge-fieldlike nature of the nematic fluctuation.[25] Just like electromagnetic wave generated by a dipole antenna propagates in the direction transverse to the dipole moment oscillation, nematic fluctuation effect is most severe in the direction transverse to the back and forth motion of nodes. The self-energy $\hat{\Sigma}(\vec{p},\omega)$ should be computed numerically[9] unless the gap slope happens to be equal to the fermi velocity ($v_F=v_\Delta=v$), in which case $\hat{\Sigma}(\vec{p},\omega)$ has a closed-form expression:

$$\hat{\Sigma}(\vec{p},\omega) = \frac{\omega\mathbb{I} - vp_x\hat{\sigma}_3 + vp_y\hat{\sigma}_1}{3\pi^2/2}\left[\frac{2}{3} + \ln\left(\frac{\Lambda^2}{-\omega^2+v^2|\vec{p}|^2}\right)\right] \tag{5}$$

Note that the Im $\Sigma(\vec{p},\omega)$, which gives decay rate to qp with momentum $\vec{q}$ and energy $\omega$ is large and finite when there is enough energy to loose to critical fluctuations $\omega > v|\vec{p}|$. When $v_F \gg v_\Delta$ as in cuprates,[10] there is additional logarithmic contribution to the self-energy matrix which effectively flattens the gap slope further without affecting the effective fermi velocity.[9,29] [Intriguingly, systematic flattening of the gap slope with underdoping recently observed in $Bi_2Sr_2CaCu_2O_{8+\delta}$ (Refs. 2 and 20–22) could therefore be related to this effect.] As a result, the qp's at the tips no longer have sufficient energy to loose to critical fluctuations and this kinematic constraint leads to the coherence contrast. Furthermore this effect is robust against vertex corrections which were ignored in Eq. (2) effects ignored in Eq. (2). Such corrections are generally unimportant for "free" particles while they will not improve the coherence of qp's in the transverse direction that are already damaged.

The most prominent effect of nematic quantum critical fluctuations is to reveal isolated peak positions in the QPI intensity. Compare the linearized Bogoliubov qp's without and with nematic critical fluctuations in Fig. 2 demonstrates. Figure 2(a) shows extended and broad line shaped segments and the less extended but faint patterns. The vectors $\vec{q}_i$ connecting the tips of bananas shown in Fig. 1(b) are overlaid on the intensity plot in Figs. 2(b) and 2(c). Clearly, $\vec{q}_3$, $\vec{q}_4$, and $\vec{q}_7$ land on the broad line shaped segments but the rest of $\vec{q}_i$ vectors point to very faint features. This is inconsistent with

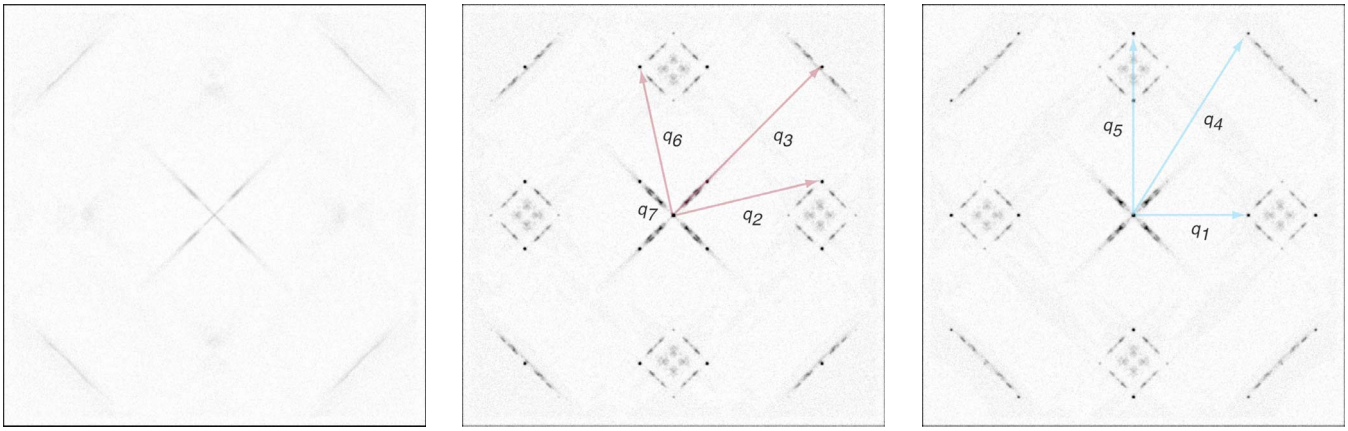


FIG. 2. (Color online) (a) QPI Fourier amplitudes $|N(q_x,q_y,\omega=9\ \text{meV})|$ for free Bogoliubov qp's with linearized dispersion. (b) QPI Fourier amplitudes at the nematic QCP in the presence of scalar (nonmagnetic) impurities ($\vec{q}_i$, $i=\{2,3,6,7\}$ label the constructively interfering peaks) (c) QPI Fourier amplitudes at the nematic QCP in the presence of magnetic impurities ($\vec{q}_i$, $i=\{1,4,5\}$ label the constructively interfering peaks). The $\vec{q}_i$ vectors, defined in Fig. 1(b) are precisely those specified in the octet model of Ref. 1. Note that at all $\vec{q}_i$ the QPI Fourier amplitudes are dramatically enhanced at the Nematic QCP. We used a gray scale where black represents intensities greater than a fixed threshold that is the same for all plots.

the experiments showing well defined peaks at all $\vec{q}_i$ vectors albeit with varying intensities. On the other hand, nematic quantum critical qp's allow for unambiguous identification of all $\vec{q}_i$ vectors. (Note that the intensity is higher for sign reversing scattering vectors $\vec{q}_2$, $\vec{q}_3$, $\vec{q}_6$, and $\vec{q}_7$ when the QPI is due to charge impurities. This is consistent with the trend observed in superconducting $Bi_2Sr_2CaCu_2O_{8+\delta}$.[1,2,8,22]) Such contrast between free qp's and nematic quantum critical qp's are more quantitatively displayed in line cuts in Fig. 3 along $\vec{q}_1$ direction and $\vec{q}_7$ direction.

Constructive and destructive interference effects in Fig. 2(b) further signifies the interference origin of the peaks. There are two classes of scattering $\vec{q}_i$ vectors connecting $\vec{k}$ space points in a $d$-wave superconductor, depending on whether they connect points with the opposite sign of the gap [q2, q3, q6, q7 (red) in Figs. 1 and 2] or the same sign of the gap [q1, q4, q5 (blue) in the same figures]. Each of these classes of $\vec{q}_i$ vectors can be associated with constructive or destructive interference depending on the nature of the impurity scattering center.[13,14] For the charged impurity potential which is asymmetric in Nambu space (charged impurities affect particles and holes differently), *sign reversing* $\vec{q}_i$'s are expected to yield constructive interference. On the other hand, both magnetic impurities $V_m\mathbb{I}$ and pair scattering centers $V_\Delta\hat{\sigma}_1$ which are symmetric in Nambu space are expected to yield constructive interference for *sign-preserving* $\vec{q}_i$'s. What is new here is that nematic critical fluctuations clearly reveal the octet peaks through the accumulation of coherence at the tips in the $\vec{k}$ space equal-energy contour, and hence enable sharp comparison between QPI's induced by different types of impurity scattering centers. This reasoning is clearly borne out in the line cuts (Fig. 3).

One way of tuning the degree of such constructive and destructive interference is to introduce vortices. A vortex can act both as a pair field impurity due to its core and as a magnetic impurity due to screening currents. Since both the pair field impurity and magnetic impurity are symmetric in

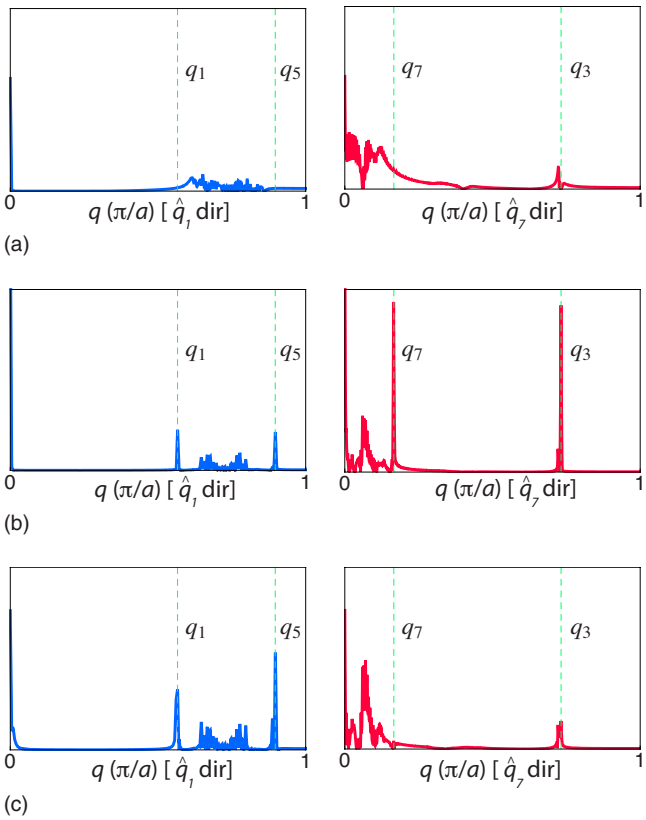


FIG. 3. (Color online) Normalized LDOS line cuts of the interference signal along the $\vec{q}_1$ (or the [100]) direction and along the $\vec{q}_7$ (or [110]) direction. All plots have the same $y$-axis scale. (a) weak features of a BCS $d$-wave superconductor. At the nematic QCP (b) shows scalar impurities inducing constructive interference at $\vec{q}_1$ and $\vec{q}_5$, and destructive interference at $\vec{q}_3$ and $\vec{q}_7$ while (c) shows the opposite behavior for the case of magnetic impurities. QPI due to a pairing impurity $V_\Delta\hat{\sigma}_1$ has a qualitatively similar pattern to (c) (not presented).

Nambu space, vortices would shift the QPI intensity toward sign-preserving vectors as shown in Figs. 2(c) and 3(c). This trend is in remarkable agreement with recent unpublished magnetic field dependence studies of QPI by *T*. Hanaguri *et al.*[30] Scattering due to thermally excited vortices should also lead to a similar trend of enhancing peaks at $\vec{q}_1$, $\vec{q}_4$, and $\vec{q}_5$ upon raising temperature.

In summary, we have shown that nematic critical fluctuations provide a natural mechanism for the accumulation of coherence that can lead to well defined peaks in the QPI map in a manner that is consistent with the existing experimental literature. Octet vectors $\vec{q}_i$ were unmistakably revealed through a straightforward calculation. One open question is how to resolve the disappearance of the dispersing QPI peaks that accompanies the emergence of nematic glass features at high energy scales.[2,22] This is a subject for future study. Perhaps the most tantalizing question one could ask would be whether nematic quantum critical fluctuations provide the unique mechanism for the existence of dispersing QPI peaks. If the octet peaks in cuprate are indeed evidence of nematic fluctuation, they will disappear in the isotropic phase which is likely to be the overdoped regime. We also expect the contrast for dispersing signals in FT-STS to weaken at energy scales below $T_n$ (i.e., outside the quantum critical regime, see Fig. 1).

We thank J. C. Davis, E. Fradkin, J. E. Hoffman, S. Kivelson, T. Pereg-Barnea, S. Sachdev, J. Sethna, K. Shen, O. Vafek, and A. Balatsky for useful discussions. We thank T. Hanaguri for discussions and sharing his data prior to publication.

[1] K. McElroy, R. W. Simmonds, J. E. Hoffman, D. H. Lee, J. Orenstein, H. Eisaki, S. Uchida, and J. C. Davis, Nature (London) **422**, 592 (2003).
[2] Y. Kohsaka *et al.*, Nature (London) **454**, 1072 (2008).
[3] N. Doiron-Leyraud, C. Proust, D. LeBoeuf, J. Levallois, J.-B. Bonnemaison, R. Liang, D. A. Bonn, W. N. Hardy, and L. Taillefer, Nature (London) **447**, 565 (2007).
[4] S. E. Sebastian, N. Harrison, E. Palm, T. P. Murphy, C. H. Mielke, R. Liang, D. A. Bonn, W. N. Hardy, and G. G. Lonzarich, Nature (London) **454**, 200 (2008).
[5] C. Howald, R. Fournier, and A. Kapitulnik, Phys. Rev. B **64**, 100504(R) (2001).
[6] K. Lang, V. Madhavan, J. Hoffman, E. Hudson, H. Eisaki, S. Uchida, and J. Davis, Nature (London) **415**, 412 (2002).
[7] M. Vershinin, S. Misra, S. Ono, Y. Abe, Y. Ando, and A. Yazdani, Science **303**, 1995 (2004).
[8] Y. Kohsaka *et al.*, Science **315**, 1380 (2007).
[9] E.-A. Kim, M. J. Lawler, P. Oreto, S. Sachdev, E. Fradkin, and S. A. Kivelson, Phys. Rev. B **77**, 184514 (2008).
[10] M. Chiao, R. W. Hill, C. Lupien, L. Taillefer, P. Lambert, R. Gagnon, and P. Fournier, Phys. Rev. B **62**, 3554 (2000).
[11] M. F. Crommie, C. P. Lutz, and D. M. Eigler, Nature (London) **363**, 524 (1993).
[12] L. Capriotti, D. J. Scalapino, and R. D. Sedgewick, Phys. Rev. B **68**, 014508 (2003).
[13] Q.-H. Wang and D.-H. Lee, Phys. Rev. B **67**, 020511(R) (2003).
[14] T. Pereg-Barnea and M. Franz, Phys. Rev. B **68**, 180506(R) (2003).
[15] A. V. Balatsky, I. Vekhter, and J.-X. Zhu, Rev. Mod. Phys. **78**, 373 (2006).
[16] T. S. Nunner, W. Chen, B. M. Andersen, A. Melikyan, and P. J. Hirschfeld, Phys. Rev. B **73**, 104511 (2006).
[17] C. Bena, S. Chakravarty, J. Hu, and C. Nayak, Phys. Rev. B **69**, 134517 (2004).
[18] M. Vojta, Y. Zhang, and S. Sachdev, Phys. Rev. Lett. **85**, 4940 (2000).
[19] V. Hinkov, D. Haug, B. Fauque, P. Bourges, Y. Sidis, A. Ivanov, C. Bernhard, C. T. Lin, and B. Keimer, Science **319**, 597 (2008).
[20] K. Tanaka *et al.*, Science **314**, 1910 (2006).
[21] M. Le Tacon, A. Sacuto, A. Georges, G. Kotliar, Y. Gallais, D. Colson, and A. Forget, Nat. Phys. **2**, 537 (2006).
[22] J. W. Alldredge *et al.*, Nat. Phys. **4**, 319 (2008).
[23] J.-X. Zhu, K. McElroy, J. Lee, T. P. Devereaux, Q. Si, J. C. Davis, and A. V. Balatsky, Phys. Rev. Lett. **97**, 177001 (2006).
[24] T. Pereg-Barnea and M. Franz, Phys. Rev. B **78**, 020509(R) (2008).
[25] P. G. de Gennes and J. Prost, *The Physics of Liquid Crystals* (Oxford Science Publications, New York, 1995).
[26] K. McElroy, G.-H. Gweon, S. Y. Zhou, J. Graf, S. Uchida, H. Eisaki, H. Takagi, T. Sasagawa, D.-H. Lee, and A. Lanzara, Phys. Rev. Lett. **96**, 067005 (2006).
[27] J. R. Schrieffer, *Theory of Superconductivity* (Westview Press, Boulder, CO, 1999).
[28] M. R. Norman, M. Randeria, H. Ding, and J. C. Campuzano, Phys. Rev. B **52**, 615 (1995).
[29] Y. Huh and S. Sachdev, Phys. Rev. B **78**, 064512 (2008).
[30] T. Hanaguri, Y. Kohsaka, M. Ono, M. Maltseva, P. Coleman, I. Yamada, M. Azuma, M. Takano, K. Ohishi, and H. Takagi, Science **323**, 923 (2009).